Coerced Coarsening of Nanoparticle Assemblies: A Mechanical Drive Towards Equilibrium

M. O Blunt,[1] C. P. Martin,[1] M. Ahola-Tuomi,[2] E. Pauliac-Vaujour,[1]
P. Sharp,[1] P. Nativo,[3] M. Brust,[3] and P. Moriarty[1]

[1] *The School of Physics and Astronomy, The University of Nottingham, Nottingham NG7 2RD, UK*
[2] *Department of Physics, University of Turku, FIN-20014 Turku, Finland*
[3] *Centre for Nanoscale Science, University of Liverpool, Crown Street, Liverpool L69 7ZD, UK*

Coarsening is a ubiquitous phenomenon[1–3] which underpins countless processes in Nature including epitaxial growth[1,3,4]; the phase separation of alloys, polymers, and binary fluids[2]; the growth of bubbles in foams[5]; and pattern formation in biomembranes[6]. Here we show, in the first real time experimental study of the evolution of an adsorbed colloidal nanoparticle array, that tapping mode atomic force microscopy can drive the coarsening of Au nanoparticle assemblies on silicon surfaces. Although the growth exponent has a strong dependence on the initial sample morphology, our observations are largely consistent with modified Ostwald ripening processes[7–9]. To date, ripening processes have been exclusively considered as thermally-activated but we show that nanoparticle assemblies can be *mechanically* coerced towards equilibrium, representing a new approach to directed coarsening. This strategy enables precise control over the evolution of micro- and nanostructures.

In our experiments, tapping mode atomic force microscopy (TM-AFM) is used to both drive and monitor the evolution of 2D nanoparticle arrays (see Methods). Self-organisation in colloidal nanoparticle systems gives rise to a panoply of intricate patterns[10–15] and the dynamics of the self-organisation process have been investigated[11,14–16]. In one case, a quench-and-observe strategy has been used to ascertain the value of the coarsening exponent, γ for the time-dependent growth of clusters of PbSe nanoparticles[11]. As compared to that study, the mechanically driven evolution we observe (via a 'real time' study)) is associated with a markedly different scaling exponent. Moreover, we show that the value of the growth exponent arising from probe-driven coarsening has a strong dependence on whether the initial sample morphology comprises isolated clusters or "labyrinthine" assemblies.

Octanethiol-passivated Au nanoparticles were prepared in toluene using the method pioneered by Brust et al.[17]. Small angle X-ray scattering at the XMaS beamline of the European Synchrotron Radiation Facility (ESRF) was used to characterise the average nanoparticle diameter (2.0 nm) and size distribution ($\pm 8\%$). The solvent was then allowed to evaporate from a small volume of the nanoparticles-in-toluene solution and the particles re-dissolved in nonane. (We find that the coarsening effect we observe is much more pronounced for nanoparticles dissolved in simple alkanes as compared to toluene. Tentatively, we ascribe this effect to the presence of tetra-octylammonium bromide impurities in the original toluene-based solution[18] which are not soluble in nonane. Recent experiments with purified toulene-based nanoparticle solutions appear to support this tentative proposal). A 25 μl droplet of an appropriately diluted solution was then placed on a native oxide-terminated Si(111) substrate and the sample subsequently span at 4 krpm. The nanoparticle concentration was varied to produce either 'spinodal' or 'islanded' sample morphologies. An Asylum Research MFP-3D atomic force microscope (AFM) system operating in intermittent contact mode with closed loop control was used to image (and drive) the evolution of the resulting nanoparticle assemblies. Olympus AC240 silicon probes (spring constant: 2 Nm^{-1} and resonant frequency: 70 kHz) were used to acquire the data shown in Figs. 1 and 2. Stiffer Olympus cantilevers (AC160) were also used in some experiments (see Supplementary Information).

We first focus on the evolution of spinodal/labyrinthine assemblies. Figs. 1(a)-(d) show snapshots from a TM-AFM movie (Supplementary Information (SI), Video 1) where a striking coarsening of the assembly, qualitatively identical to that expected for an exclusively thermally-driven process, is seen to occur. For dynamic scaling to hold, the morphology of the system at a given point in time is characterised by a single length scale, $L(t)$. The evolution of the radially averaged Fourier transform of the system, $S(k,t)$, following an initial transient, should then be of the form[1,8]:

$$S(k,t) = k_{max}(t)^{-2} F(k/k_{max}(t)) \qquad (1)$$

where, k_{max} is the peak position of the structure function and $F(k/k_{max}(t))$ is a time-independent master function. To check for the presence of dynamic scaling we have therefore plotted $S(k,t)$ taken throughout the experimental run of Figure 1 (see also SI Video 2) according to Equation 1. As shown in Fig. 1(f), the structure functions each collapse almost perfectly onto a single time-invariant master curve.

That the system evolution we observe is not simply due to natural - i.e. solely thermal - coarsening and arises from probe-induced nanoparticle transport is clear from Fig. 1(e). In this image we show the boundary between a continuously scanned surface region and the surrounding region (which has been scanned only once to acquire Fig. 1(e)). The boundary is seamless. Use of a higher spring constant cantilever produces a much more rapid evolu-

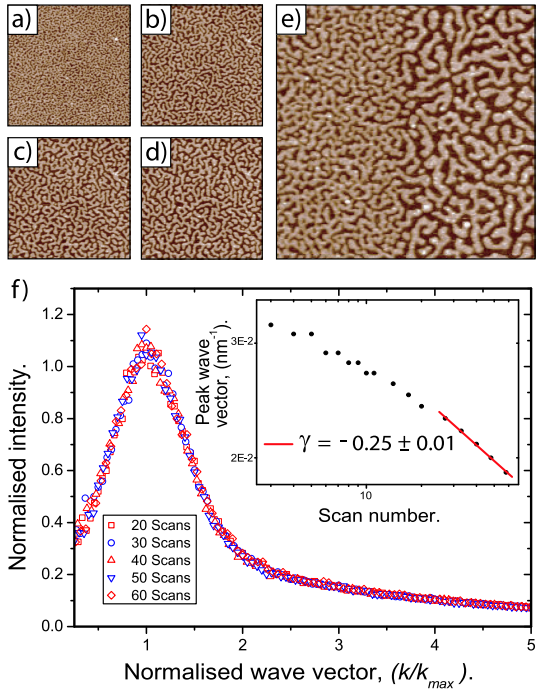

FIG. 1: Coerced coarsening of a nanoparticle assembly. **a - d** are frames (1 μm^2) from an AFM movie (Supplementary Material, Movie 1) of the evolution of a 0.55 monolayer (ML) coverage of nanoparticles over the course of 8 hours of scanning. Each frame is separated in time by $\sim$ 2 hours. The labyrinthine morphology results from solvent evaporation in the spinodal limit and is thus associated with a well-defined spatial correlation. In **e**, a striking delineation between the probe-coarsened region following a total of 8 hours imaging and the surrounding surface (scanned once, left hand side of the image) is observed. Dynamic scaling is clear from **f** where radially-averaged Fourier transforms taken at various intervals can be re-scaled to collapse onto a time-independent master curve.

tion of the system (SI, Video 3). It is also important to note that the total mass of the nanoparticle assembly is conserved throughout the coarsening process.

The probe-induced dynamic we observe is noteworthy from a number of perspectives. The system retains a remarkable level of self-similarity throughout its coarsening meaning that *a given length scale can be selected simply by halting the imaging process at an appropriate point.* It is also striking that in very many cases the system morphology remains isotropic (see Fig. 1). Given the raster nature of the scan process, however, one might ask why strongly anistropic structures (see SI, Videos 4 and 5) are not *exclusively* formed? We find that well-defined anisotropic structure forms only in spinodal assemblies and, even then, qualitatively similar initial morphologies lead to very different levels of anisotropy (compare SI Videos 1 and 4). We return to the question of anisotropy in the final paragraph.

The inset to Fig. 1(f) shows that the coarsening exponent, γ, asymptotically approaches a value of 0.25 $\pm$ 0.01 for the morphological evolution in Figs. 1(a)-(d) and SI Video 1. Rabani et al.[11] have shown that the coarsening of PbSe nanoparticle islands follows a $t^{\frac{1}{4}}$ dependence consistent with a cluster diffusion-coalescence process. We have used the Rabani et al. Metropolis algorithm[13] to investigate the dynamics of coarsening of a 'spinodal' nanoparticle assembly. The simulation yields a scaling exponent of $\frac{1}{4}$, in excellent agreement with the experimental data. Importantly, however, an exponent of $\frac{1}{4}$ has also been attributed to Ostwald ripening[19] - the net transfer of monomers from smaller to larger islands - of a spinodal structure mediated by mass transport along domain boundaries[8].

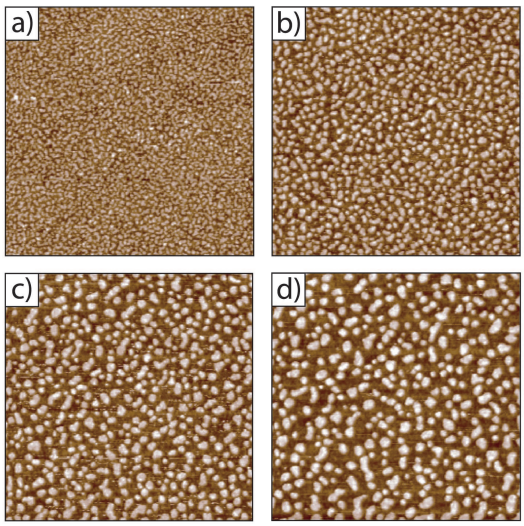

FIG. 2: Evolution of an ensemble of nanoparticle islands. Each of frames **a** - **d** is 1 μm^2 in area with a total of $\sim$ 2 hours of scanning between frames. (All frames are taken from Supplementary Material, Movie 4). Note the presence of substantial streaking in **c**.

As the form of the island size distribution function can be more sensitive to the coarsening mechanism than a power law exponent alone, deeper physical insight can be obtained from a consideration of the evolution of samples comprising an ensemble of isolated islands. (Fig 2 and SI, Movie 6). As shown in Fig. 3(a), the value of γ exhibits an abrupt change from a value of $\sim$ 0.1 to, at approximately scan number 20, a value of 0.49 ± 0.02. This transient behaviour betrays an important contribution to the probe-induced coarsening mechanism. In Fig.3(b) we plot data for a sample having an initial morphology close to that of Fig. 2 but where a transition to a coarsening exponent of $\sim \frac{1}{2}$ is not observed. This apparent inconsistency in the experimental data can be explained by reference to the insets of Fig. 3(a) and Fig. 3(b). As, in our case, the tip radius of curvature is substantially greater than that of a single nanoparticle, individual particles comprising the aggregates are not resolved. The average height thus provides a measure of the degree of close-packing within an island. In Fig. 3(a) the

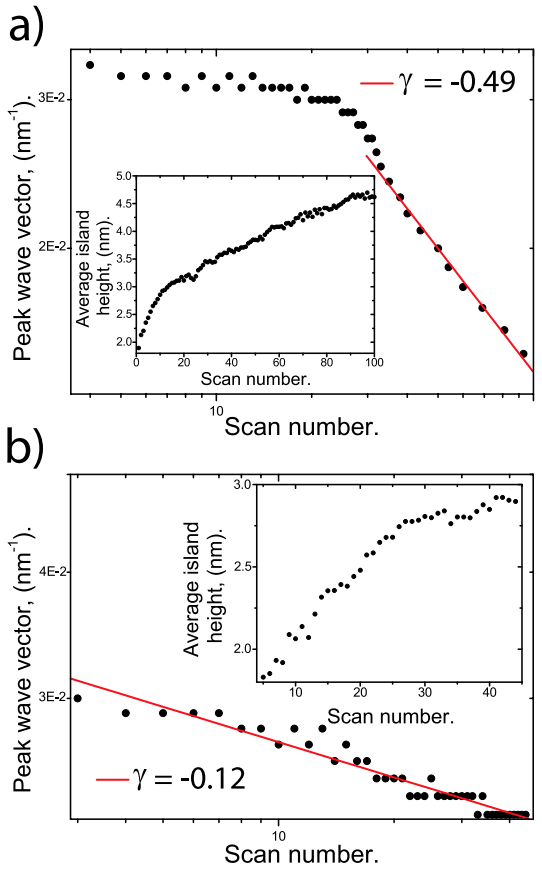

FIG. 3: Change in the position of the peak in the radially averaged Fourier transform of images of evolving ensembles of nanoparticle islands. **a** shows the data associated with Fig. 2 (and Movie 4) whereas **b** was acquired from a different sample with a morphology very similar to that shown in Fig. 2(a). A sharp transition in the value of γ is seen in the inset to **a** which correlates very closely with an abrupt change in the gradient of mean island height vs scan number. This threshold island height (i.e. nanoparticle density) is not reached in

sharp transition in the value of γ is matched directly by an abrupt change in the slope of the average height vs. scan number curve. This occurs for Fig. 3(a) at $\sim$ scan number 20 and at a "threshold" apparent height of $\sim$ 3.2 nm. For the data of Fig. 3(b), the threshold height is not reached and the system remains in the transient regime. We can therefore infer that a significant percentage of the force exerted by the AFM probe in the initial scans drives the nanocrystals into more densely packed arrangements. Only when this initial packing phase induces a threshold density can the coarsening models described above be reliably applied.

The exponent of $\frac{1}{2}$ from Fig. 3(a) is expected on the basis of detachment/attachment-limited Ostwald ripening[20]. Detachment-limited kinetics are fully consistent with the mechanical coarsening process we observe: the rate-limiting step is not (probe-induced) diffusion but the detachment(attachment) of a nanoparticle from(to) the edge of an island. Furthermore, a close examination of SI Movie 6 shows that two key processes occur: (i) a gradual shrinkage of smaller islands until they disappear (with no obvious collisions occurring), and (ii) coalescence of islands via the growth of neighbouring (and expanding) clusters "into" each other. As pointed out by Wen et al.[21] these observations are consistent with an Ostwald ripening process.

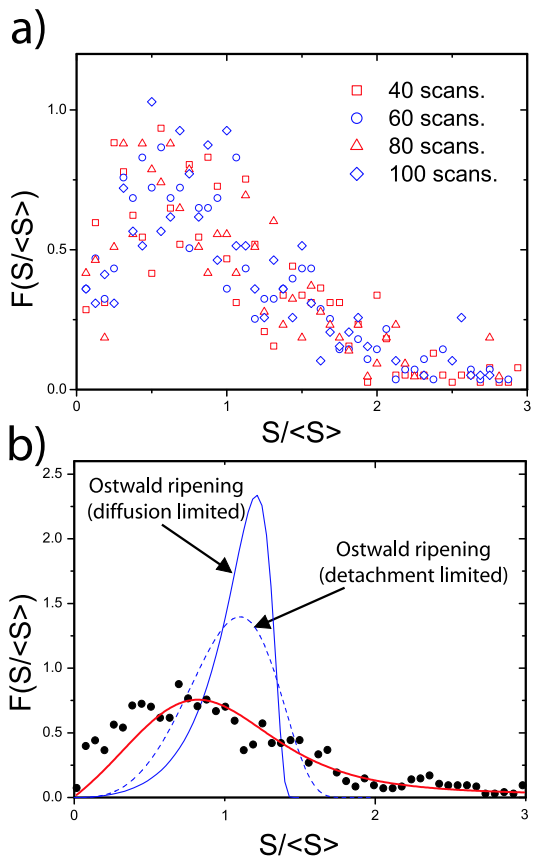

FIG. 4: Scaled island size distributions for a nanoparticle island ensemble subject to mechanically-driven coarsening. **a** shows the distributions at a number of different points (in time) in the coarsening of the ensemble. The averaged scaled distribution (shown as the data points in **b**) can be fit with an approximate form proposed by Conti et al.[9] for Ostwald ripening which takes into account binary coalescence events. Note that the standard Lifshitz-Slyozov[22] (solid blue line) and Wagner[20] (dashed line) distribution functions lack the pronounced tail produced by binary coalescence.

Further evidence for Ostwald ripening is provided by a consideration of the distribution of the (linear) sizes of the nanoparticle islands. Normalised size distributions, $F(s/<s>)$ vs $s/<s>$, (where $<s>$ is the average linear island size for a given image) for various frames of Movie 6, following the transition at scan number 20 discussed above, are shown in Fig. 4(a). Although there is significant scatter in the data, it is clear that the functional form of the distribution curve is preserved throughout the coarsening process. To improve the statistics we

have therefore averaged the island size distributions for the final ten frames and plotted this as the data points in Fig. 4(b). Note that the experimental data exhibit a long tail towards *higher* values of the normalised radius. This long tail is not predicted by Wagner's mean-field theory of detachment-limited Ostwald ripening[20] (shown as the dashed line in Fig. 4(b)).

We can account for the skew towards higher values of normalised radius by realising that the island ensemble of Fig. 2 (and SI Movie 6) is far from the limit of vanishing area fraction required for the mean-field approximation. Conti et al.[9] have shown that an approximate solution for the scaled island distribution arising from Ostwald ripening combined with binary coalescence is as follows:

$$F(s_n) = \frac{s_n}{(s_n^2 - 2\beta s_n + 2)^2} \times exp\left(-\frac{2\beta}{\sqrt{2-\beta^2}} arctan(\frac{s_n - \beta}{\sqrt{2-\beta^2}})\right) \quad (2)$$

where s_n is the normalised radius, and β is a constant. We have fitted Equation 2 to our experimental data with the result shown in Fig. 4(b). Given that Eqn. 2 represents an approximate solution to the distribution function, the fit is reasonable and certainly describes the tail to high values of normalised radius very well.

Finally, we return to the question of anisotropy. Extraction of growth exponents in orthogonal directions requires, in our case, a determination of the mean width and length of very irregular worm-like domains (see SI Movie 4). This is problematic at best as the islands do not conform to the simple rectangular shape considered in previous work on anisotropic coarsening[23,24]. Crude estimates of mean island lengths and widths suggest that the growth exponents for the major and minor axes of the islands do not differ substantially (within experimental error) although there is some evidence to suggest that the island width saturates in the latter stages of coarsening[25]. From the measurements of ensembles of isolated islands with close to circular symmetry (SI Movie 6) it is clear that with a suitable starting morphology nanoparticle clusters can relax to a less elongated configuration during coarsening, despite the highly anisotropic nature of the probe-induced diffusion process. Future work will focus on elucidating the relative roles of probe-driven anisotropic diffusion and relaxation dynamics using fast (MHz) sampling of the SPM cantilever signal.

I. ACKNOWLEDGEMENTS

We are grateful for the financial support of the U.K. Engineering and Physical Sciences Research Council and the EU Framework Programme 6 Marie Curie Research Training Networks scheme (under grant MRTN-CT-2004005728 (PATTERNS)). The grazing incidence small angle x-ray scattering work was performed on the EPSRC-funded XMaS beam line at the ESRF, directed by M.J. Cooper and C. Lucas. We are grateful to the beam line team of S.D. Brown, L. Bouchenoire, D. Mannix, D.F. Paul and P. Thompson for their invaluable assistance, and to Mark Everard, Chris Nicklin, and Richard Williams for both collaborating on the SAXS experiments and for helpful advice related to nanoparticle synthesis. We also would like to very gratefully acknowledge extremely helpful discussions with Paul Mulheran, Juan P. Garrahan, and members of the PATTERNS RTN (in particular, Uwe Thiele and Ulli Steiner).

[1] *Phase Transitions and Critical Phenomena*, edt. C. Domb & JL Lebowitz (Academic, New York, 1983), Vol. 3.

[2] Furukawa, H. A dynamic scaling assumption for phase separation. *Adv. Phys.* **34**, 703 - 750 (1985).

[3] Bray, A.J. Coarsening dynamics of phase-separating systems. *Phil. Trans. Roy. Soc. London A* **361**, 781-791 (2003).

[4] Zinke-Allmang, M. Phase separation on solid surfaces: nucleation, coarsening, and coalesence kinetics. *Thin Solid Films* **346** 1 - 68 (1999).

[5] Glazier, J.A. & Weaire D. The kinetics of cellular patterns. *J. Phys. Cond. Matt.* **4** 1867 (1992).

[6] John, K. & Bar, M. Alternative mechanisms of structuring biomembranes:Self-assembly versus Self-organisation. *Phys. Rev. Lett.* **95** 198101 (2005).

[7] Huse, D. A. Corrections to late-stage behaviour in spinodal decomposition: Lifshitz-Slyozov scaling and Monte Carlo simulations*Phys. Rev. B* **34**, 7845 (1986).

[8] Ernst, H.-J., Fabre F., & J. Lapujoulade. Observation of dynamic scaling in "spinodal decomposition" in two dimensions. *Phys. Rev. Lett.* **69**, 458 (1992).

[9] Conti, M., Meerson, B., Peleg A. & Sasorov P. V. Phase ordering with a global conservation law: Ostwald ripening and coalescence. *Phys. Rev. E* **65**, 046117 (2002).

[10] Ge, G. & Brus, L. Evidence for spinodal phase separation in two-dimensional nanocrystal self-assembly. *J. Phys. Chem. B* **104**, 9573 (2000).

[11] Rabani, E., Reichman, D. R., Geissler, P. L. & Brus, L. E. Drying-mediated self-assembly of nanoparticles. *Nature* **426**, 271 - 274 (2003).

[12] Moriarty, P., Taylor, M. D. R., & Brust, M. Nanostructured cellular networks. *Phys. Rev. Lett* **89** 248303-1 - 248303-4 (2002).

[13] Martin, C. P., Blunt, M. O. & Moriarty, P. Nanoparticle networks on silicon: self-organised or disorganised? *Nano Lett.* **4**, 2389 (2004).

[14] Narayanan, S., Wang. J & Lin, X. -M. Dyanmical self-assembly of nanocrystal superlattices during colloidal droplet evaporation by in situ small angle X-ray scat-

tering. *Phys. Rev. Lett.* **93**, 135503 (2004).

[15] Bigioni, T. P., Lin, X.-M., Nguyen, T. T., Corwin E. I., Witten T. A., and Jaeger H. M. Kinetically driven self assembly of highly ordered nanoparticle monolayers. *Nature Mat.* **5**, 265 (2006).

[16] Sztrum, C. G. & Rabani, E. Out-of-equilibrium self-assembly of binary mixtures of nanoparticles. *Adv. Mat.* **18** 565 (2006).

[17] Brust M., Walker M., Bethell D., Schiffrin D. J. & Whyman, R. Synthesis of thiol-derivatised gold nanoparticles in a 2-phase liquid-liquid system. *J. Chem. Soc. Chem. Comm.* **7**, 801 (1994).

[18] Waters, C. A., Mills, A. J., Johnson, K. A. & Schiffrin, D. J. Purification of dodecanethiol derivatised gold nanoparticles. *Chem. Comm.* **4**, 540 (2003).

[19] Ostwald, W. *Z. Phys. Chem.* **37** 385 (1901).

[20] Wagner, C. Theorie dealtering von Niederschlgen durch umlösen *Z. Elektrochem.* **65**, 581 (1961).

[21] Wen, J.-M., Evans, J. W., Bartelt, M. C., Burnett, J. W. & Thiel, P.A. Coarsening mechanisms in a metal film: From cluster diffusion to vacnacy ripening, *Phys. Rev. Lett.* **76**, 652 (1996).

[22] Lifshitz, I.M. & V. V. Slyozov. The kinetics of precipitation from supersaturated solid solutions. *J. Phys. Chem. Sol.* **19**, 35 (1961).

[23] Morgenstern, K., Laegsgaard, E., Stensgaard I.& Besenbacher F. Transition from One-Dimensional to Two-Dimensional Island Decay on an Anisotropic Surface, *Phys. Rev. Lett.* **83**, 1613 (1999).

[24] Yao, Y., Ebert, Ph., Li, M, Zhang, Z. & Wang E. G. Decay characteristics of two-dimensional islands on strongly anisotropic surfaces, *Phys. Rev. B* **66**, 041407(R) (2002).

[25] Blunt, M.O., Martin, C.P., Vaujour, E. & Moriarty, P. J., unpublished.